

# Design Methodology for Microelectromechanical Systems. Case Study: Torsional Scanner Mirror

Faik Can Meral

Ipek Basdogan

Department of Mechanical Engineering,  
Koc University,  
Sariyer, Istanbul 80910, Turkey

*Future optical microsystems, such as microelectromechanical system (MEMS) scanners and micromirrors, will extend the resolution and sensitivity offered by their predecessors. These systems face the challenge of achieving nanometer precision subjected to various disturbances. Predicting the performance of such systems early in the design process can significantly impact the design cost and also improve the quality of the design. Our approach aims to predict the performance of such systems under various disturbance sources and develop a generalized design approach for MEMS structures. In this study, we used ANSYS for modeling and dynamic analysis of a torsional MEMS scanner mirror. ANSYS modal analysis results, which are eigenvalues (natural frequencies) and eigenvectors (mode shapes), are used to obtain the state-space representation of the mirror. The state-space model of the scanner mirror was reduced using various reduction techniques to eliminate the states that are insignificant for the transfer functions of interest. The results of these techniques were compared to obtain the best approach to obtain a lower order model that still contains all the relevant dynamics of the original model. After the model size is reduced significantly, a disturbance analysis is performed using Lyapunov approach to obtain root-mean-square values of the mirror rotation angle under the effect of a disturbance torque. The magnitude levels of the disturbance torque are obtained using an experimental procedure. The disturbance analysis framework is combined with the sensitivity analysis to determine the critical design parameters for optimizing the system performance. [DOI: 10.1115/1.2756087]*

## 1 Introduction

Microsystems design and manufacturing technology are developing rapidly. There are a variety of specialized computer aided design tools in the microelectromechanical system (MEMS) area, such as SUGAR [1] and ANSYS [2]. Although these tools can provide a lot of insight into the design of MEMS devices, they are limited with the built-in algorithms. These algorithms are not expandable if the user wants to do further analysis. For conceptual design, there are a few existing design synthesis studies. Li and Antonsson [3] developed an approach for automatic synthesis of MEMS mask layouts. Mukherjee and Fedder [4] have presented a structured design method for MEMS. Other examples include the automated design synthesis method for MEMS by Zhou et al. [5]. Deshpande and Saggere [6] used analytical and finite element models to obtain the key dimensions of a microactuator through design optimization. Sensitivity analysis is one of the design techniques that can be used to identify the critical design parameters for optimizing the performance of a system. Sensitivity information provides the performance change of a system with respect to changing design parameters. In a previous work by Shi et al. [7], sensitivity analysis was carried out using the direct differentiation approach to compute the design sensitivity coefficients. The coupled electromechanical design sensitivities were studied for a reliability based analysis by Allen et al. [8]. Additionally, Sigmund [9] presented the use of sensitivity analysis for topological optimization of electromechanical systems. In another study by

Lusk and Howell [10], the different properties of the mechanisms were explored in the design space to improve the fabrication process.

Our approach aims to integrate some of the existing analysis tools and develop a generalized design approach for MEMS structures. The design methodology incorporates tools for analyzing end-to-end system performance and sensitivity of design parameters. Our integrated design approach starts with the generation of finite element model (FEM) of the MEMS structure using ANSYS software (see Fig. 1). The state-space representation of the system is constructed in MATLAB using ANSYS results. The state-space model is reduced using some reduction techniques, which will be outlined in the following section. The reduction algorithms are carefully chosen to keep the significant states for the transfer functions of interest. After developing a reduced model of the system, the next step is to predict the system performance under anticipated disturbance conditions. Section 3 outlines the disturbance analysis framework. Disturbance levels are measured experimentally and used in the disturbance analysis framework. The disturbance analysis is conducted using the Lyapunov approach. The disturbance analysis results tell us whether the system is able to meet the design requirements or not. If the requirements are met, we may consider building the prototype of our MEMS design. If the requirements are not met, then the designer can perform a sensitivity analysis. Sensitivity analysis results can be used to identify the critical design parameters for optimizing the system performance. After the critical design parameters are identified, required changes are made and the design process continues until the requirements are met.

The developed methodology is demonstrated through a case study which includes the disturbance analysis and sensitivity analysis of a torsional MEMS scanner mirror. A microscanner is a tiny movable mirror that can scan or steer a laser beam in 1D, 2D,

Contributed by the Design Theory and Methodology Committee of ASME for publication in the JOURNAL OF MECHANICAL DESIGN. Manuscript received May 4, 2006; final manuscript received December 15, 2006. Review conducted by P. John Clarkson. Paper presented at the ASME 2005 Design Engineering Technical Conferences and Computers and Information in Engineering Conference (DETC2005), Long Beach, CA, September 24–28, 2005.

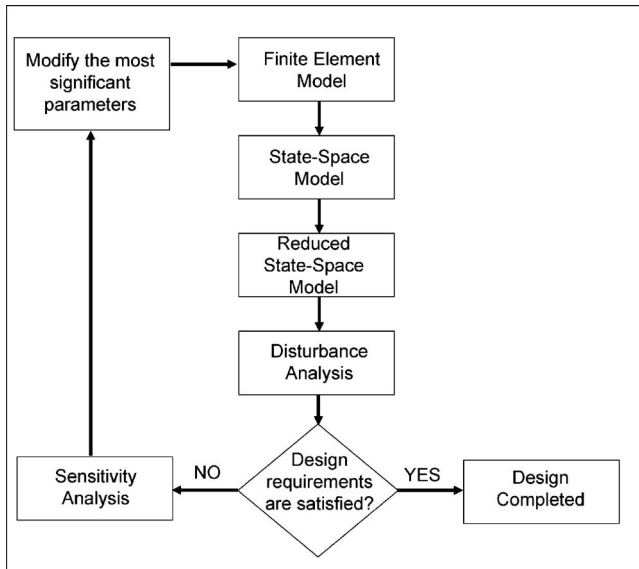


Fig. 1 Suggested design process flow for MEMS devices

or 3D. Major application areas of these mirrors can be listed as display and imaging technologies and optical switching applications in telecommunications industry [11,12]. These scanners are electromagnetically actuated. The permanent magnets on the sides create a constant magnetic field. When a current is passed through the coils on the moving plate, an in-plane electromagnetic force is exerted on the mirror, which leads to torsional deflection. In this study, the input to our system is the disturbance torque acting on the mirror about the scanning axis. The output or equivalently the performance is defined as the variation of the mirror position under the effect of a disturbance torque. The absolute value of this rotation should be kept as small as possible in order to improve the performance of the mirror.

The scanning capability of such microscanners can be significantly impacted by the disturbances coming from the outside sources. Since these devices are electrostatically or electromagnetically actuated, driving electronics jitter, control loop sensor errors and thermal changes in the environment are the examples of disturbances that may affect the performance of the mirror during the operation mode. Accurate representation of these disturbances are important in order to predict the performance of these mirrors.

In Sec. 4.1, the exact modal parameter sensitivities are calculated and compared with the sensitivities calculated using the finite difference approach (see Sec. 4.2). While these sensitivities do identify which modes are the most important, they do not reveal directly what physical characteristics of the design should be modified to affect the modes and improve the design. Physical parameter sensitivities are more intuitive, and this fact motivates to investigate the physical parameter sensitivities for the torsional MEMS scanner. Section 4.3 summarizes the physical sensitivity analysis results obtained by using the finite difference method.

The following section describes the details of the FEM of the mirror. The FEM results are then utilized to construct the state-space model which is used in disturbance and sensitivity analysis.

## 2 Finite Element Model

The FEM of the torsional scanner mirror is created in ANSYS [2]. The first model is created using the 3D solid elements and it consists of 1312 elements and 21,294 degrees of freedom (see Fig. 2(a)). The Lyapunov equation in the disturbance analysis takes excessive time for large-order systems. In order to reduce the time for the disturbance analysis, the second FEM is created using beam and shell elements, consisting of 288 elements. First five

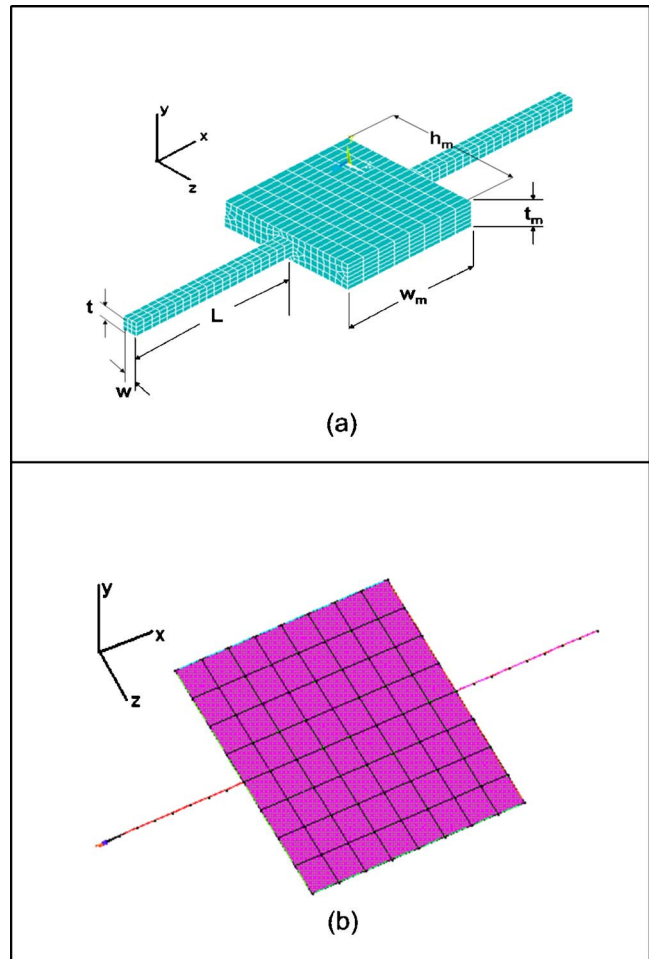


Fig. 2 Finite element models of the MEMS torsional scanner: (a) FEM with 3D solid elements showing the design parameters and (b) simplified FEM with beam and shell elements

natural frequencies are as follows: 5578, 9406, 10,664, 22,726, and 27,342 Hz.

ANSYS modal analysis results, eigenvalues and eigenvectors, are used to construct the state-space equations of the mirror. The state-space equations representing the dynamic system are [13],

$$\dot{\mathbf{x}}(t) = \mathbf{A}\mathbf{x}(t) + \mathbf{B}u(t)$$

$$\mathbf{y}(t) = \mathbf{C}\mathbf{x}(t) + \mathbf{D}u(t) \quad (1)$$

where  $\mathbf{A}$ ,  $\mathbf{B}$ ,  $\mathbf{C}$ , and  $\mathbf{D}$  are system matrices

$$\mathbf{A} = \begin{bmatrix} 0 & 1 & 0 & 0 & \dots & \dots \\ -\omega_1^2 & -2\zeta_1\omega_1 & 0 & 0 & \dots & \dots \\ 0 & 0 & 0 & 1 & \dots & \dots \\ 0 & 0 & -\omega_2^2 & -2\zeta_2\omega_2 & \dots & \dots \\ \dots & \dots & \dots & \dots & \dots & \dots \\ \dots & \dots & \dots & \dots & \dots & \dots \end{bmatrix}$$

$$\mathbf{B} = \Phi^T \begin{bmatrix} 0 \\ 1 \\ 0 \\ 1 \\ \vdots \\ \vdots \end{bmatrix} \quad \mathbf{C} = \Phi [1 \ 0 \ 1 \ 0 \ \dots \ \dots] \quad \text{and} \quad \mathbf{D} = [0] \quad (2)$$

where  $\omega_i$  is the natural frequency,  $\zeta_i$  is the damping factor, and  $\Phi$  is the modal transformation matrix obtained from the ANSYS modal analysis results.

The state-space form in the Laplace domain allows the calculation of the transfer functions  $\mathbf{H}(s)$  that relates the output rotation  $\mathbf{y}(s)$  to the given torque disturbance inputs  $\mathbf{u}(s)$ , such that

$$\mathbf{H}(s) = \frac{\mathbf{y}(s)}{\mathbf{u}(s)} \quad (3)$$

The size of the matrices can be reduced by taking only the degrees of freedom (DOFs) associated with the rotation about the flexure axis ( $x$  axis). This criterion eliminates the other modes of the system, which are associated with other DOFs. In the disturbance analysis especially the variance about the  $x$  axis is the most critical one because it is designed to work in the torsional mode. In this study, the performance is defined as the variation of the mirror position in the torsional mode. However, one can also include the other modes in the analysis if the performance criterion is changed. The results of the ANSYS modal analysis, eigenvalues and eigenvectors, were written to text files and standard MATLAB routines were used to read these files and extract the eigenvectors and eigenvalues to construct the state-space matrices.

The Lyapunov equation calculations in disturbance analysis (see Sec. 3.2) may take a long time if we use the full scale FEM. We need to reduce the size of the model while still maintaining the desired input/output relations. The MATLAB control toolbox has a function “modred,” which can be used for reducing models while retaining the overall system dc gain. The “matched dc” or “mdc” gain option for the function modred reduces the selected states by setting their derivatives to zero, and then solving for the remaining states. The other option for modred is the “del” option, which simply eliminates the defined states, typically associated with the higher frequency modes. The derivation of the mdc option is given in Ref. [14].

The alternative method is to rank the modes according to “dc gain” or “peak gain” approach. dc gain (for damped and undamped cases) is defined as

$$\text{dc gain} = \frac{y_{ji}}{u_{ki}} = \frac{y_{nji} \cdot y_{nki}}{\omega_i^2} \quad (4)$$

where  $y_{nji} \cdot y_{nki}$  is the product of the  $j$ th (output) row and  $k$ th (force applied) row terms of the  $i$ th eigenvector divided by the square of the eigenvalue for the  $i$ th mode.

At resonances, the peak gain amplitude of each mode is given by the formula

$$\text{peak gain} = \frac{y_{ji}}{u_{ki}} = \frac{-j y_{nji} \cdot y_{nki}}{2\zeta \omega_i^2} = \frac{-j}{2\zeta} (\text{dc gain}) \quad (5)$$

If the same value of  $\zeta$  is used for all modes, then all the dc gain terms are divided by the same  $2\zeta$  term and the relative amplitudes of the dc gains and peak gains are the same, so there is no difference between sorting a uniform damping model using dc gain or peak gain.

The results of the three reduction methods are shown in Figs. 3(a)–3(c). The frequency response functions in the figure show the relation between the output mirror rotation  $\mathbf{y}(s)$  to the given torque input  $\mathbf{u}(s)$ . Figure 3(a) shows the frequency response of the overall system for del modred option, where all the modes above 27,342 Hz are eliminated (only six lowest modes are kept). As it

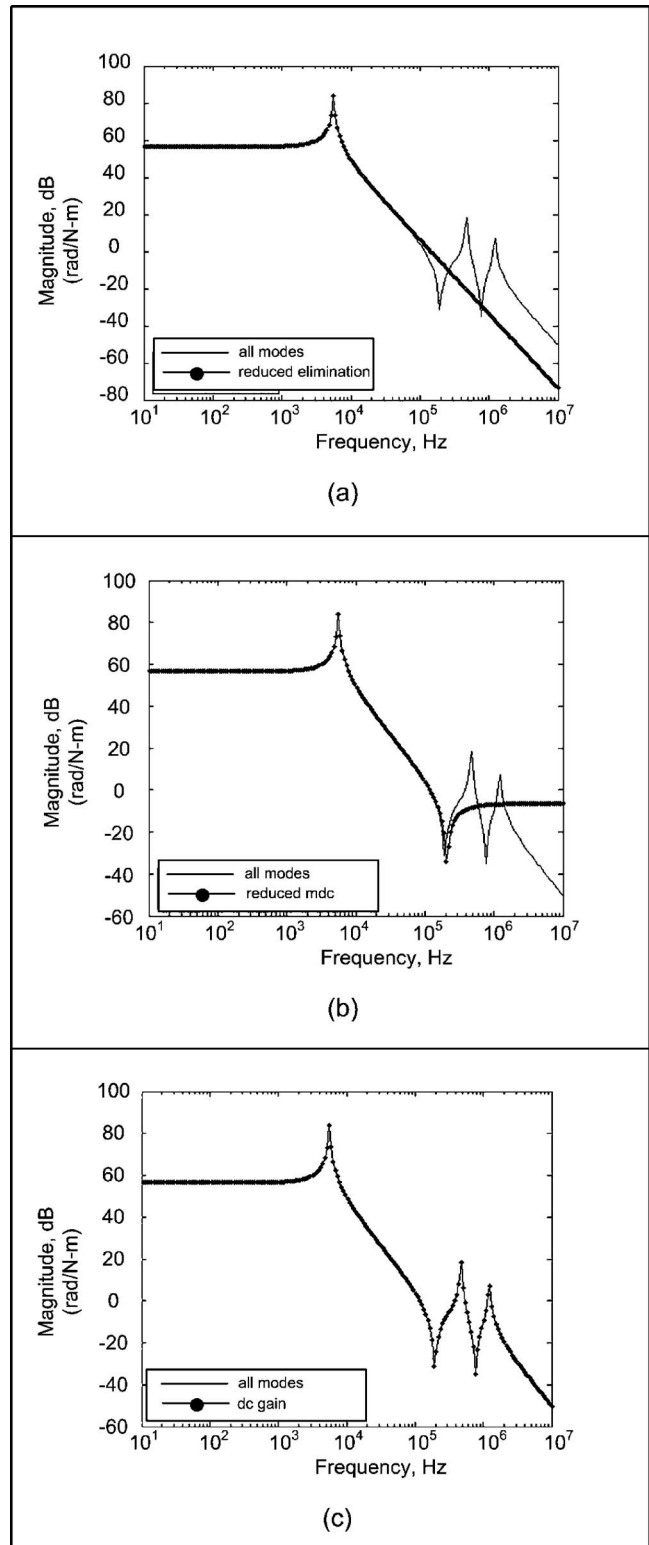


**Fig. 3 Reduced Models are obtained using (a) the first six modes, (b) “mdc” approach, and (c) “dc gain” and “peak gain” approach**

can be expected, it does not capture the higher frequency modes since they are not included in the calculations. Figure 3(b) shows the frequency response of the overall system for mdc modred option. It cannot capture the system dynamics accurately at high frequencies. Figure 3(c), shows the results of sorting the modes according to the dc gain and peak gain approach. Although the

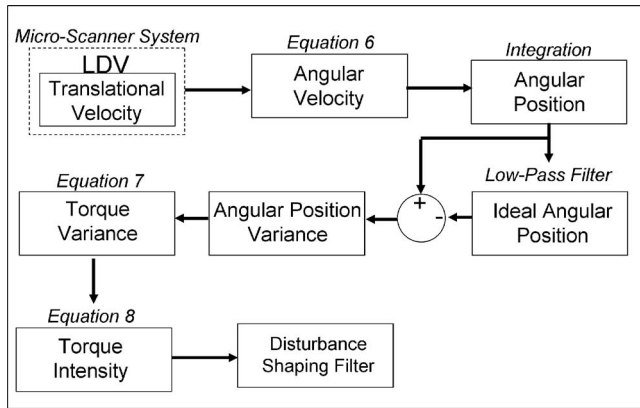


Fig. 4 Schematic of the disturbance measurement procedure

size of the state-space model has been decreased significantly (e.g., size of the matrix  $\mathbf{A}$  is reduced from  $210 \times 210$  to  $12 \times 12$ ), the reduced model captures all the significant dynamics. This method is found to be the most efficient way to reduce the state-space model of the mirror for the transfer function of interest and reduced model obtained with this technique will be used for the remaining part of this study.

### 3 Disturbance Analysis Framework

After developing a reduced model of the system, the next step is to predict the system performance under the anticipated disturbance conditions. In this section, typical environmental and sensor disturbances for a microscanner are measured experimentally and applied to the system using the Lyapunov approach. A simple lumped model in the time domain is used to validate the results. The following section summarizes the procedure and the techniques that we developed to calculate the disturbance levels acting on the microscanners.

**3.1 Characterization of the Disturbances Using Experimental Techniques.** Any unwanted effect that is coming from the environment or from the equipment can be considered as disturbance, in that it potentially interferes with the accuracy of the desired output. Development of a disturbance framework requires the real time disturbance inputs to be measured and to be modeled as precise as possible.

The experimental procedure (see Fig. 4) that we developed starts with measuring the translational velocity using a laser Doppler vibrometer (LDV). LDV is a device that measures the velocity of a moving particle using the Doppler effect [15]. LDV measures the translational velocity of a point (see Fig. 5). The mirror is actuated using a sinusoidal voltage input around its first fundamental frequency: this voltage input is converted to torque through driving electronics. The velocity output is measured using the LDV. The desired output is the angular position of the outer frame. The angular velocity of the outer frame can be calculated using the following equation:

$$V = r \times \omega \quad (6)$$

where  $V$  is the translational velocity of the point, which is read by LDV,  $\omega$  is the angular velocity of the outer frame, and  $r$  is the distance between the spot and the frame rotation axis. Note that Eq. (6) is only valid when small angle assumption is made and when the mirror is moving in pure torsional mode.

Angular velocity of the outer frame is calculated utilizing the translational velocity measured by the LDV. The next step is to integrate the velocity data in order to obtain the angular position,  $\theta$ .

Any variation from the ideal output is generated by the disturbances acting on the system. In order to obtain an ideal output for

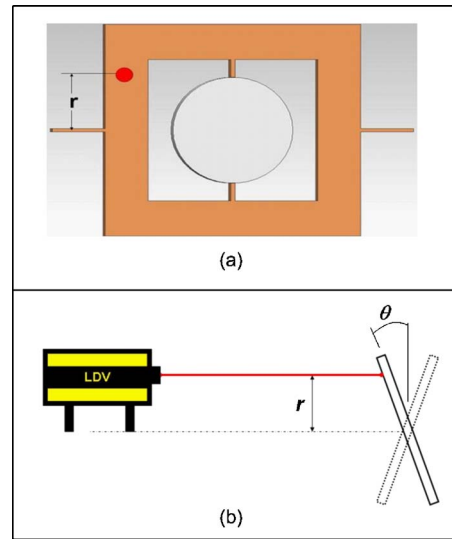


Fig. 5 (a) LDV measurement point to observe the torsional mode of the outer frame. (b) Schematic view of the LDV measurement setup (small angle  $\theta$  assumption).

mirror angular position, a low-pass filter was used to eliminate the high frequency signals from the measured data. If we subtract the “ideal” from the “measured,” that should give us the variation in the angular position.

The variation of the position (see Fig. 6(a)) is plugged into the following equation to obtain the variation in the disturbance torque (see Fig. 6(b)):

$$J_{\text{eff}} \ddot{\theta} + b \dot{\theta} + k_{\text{tors}} \theta = T_{\text{dist}} \quad (7)$$

The inertia ( $J_{\text{eff}}$ ), damping ( $b$ ), and stiffness ( $k_{\text{tors}}$ ) properties are calculated using the formulas tabulated in Tables 1 and 2 [16]. The disturbance noise intensity is defined in Ref. [17] as

$$D = \max[\Phi(\omega)] \quad (8)$$

where  $\Phi(\omega)$  is the frequency dependent power spectrum of zero-mean disturbance. The intensity of the disturbance is calculated using the above formula. The disturbance intensity for the input torque is calculated as  $1.75 \times 10^{-12}$  N m. The Lyapunov approach described in the following section is based on the “unit intensity white noise,” and this unit intensity must be scaled by the real “disturbance intensity” to simulate the actual disturbances acting on the system.

**3.2 Disturbance Analysis Using Lyapunov Approach.** For stochastic linear systems driven by white noise, the solution of the Lyapunov equation represents the variance of the state vector [18]. The disturbance torque is modeled as the output of a first order shaping filter, which is driven by unit intensity white noise [19]. The cutoff frequency of the filter is at 100 kHz such that it attenuates the frequencies above 100 kHz. The magnitude content of the disturbance shaping filter is scaled by an “intensity” constant, which was determined by experimental measurements in the previous section.

The disturbance filter can be modeled in state-space form as

$$\begin{aligned} \dot{\mathbf{x}}_d(t) &= \mathbf{A}_d \mathbf{x}_d(t) + \mathbf{B}_d \cdot \mathbf{x}_d(t) \\ u(t) &= \mathbf{C}_d \cdot \mathbf{x}_d(t) \end{aligned} \quad (9)$$

Placing this state-space system in series (see Fig. 7) with the plant equations from Eq. (1), an overall system of the form

$$\dot{\mathbf{x}}(t) = \mathbf{A}_{zd} \mathbf{x}(t) + \mathbf{B}_{zd} d(t)$$

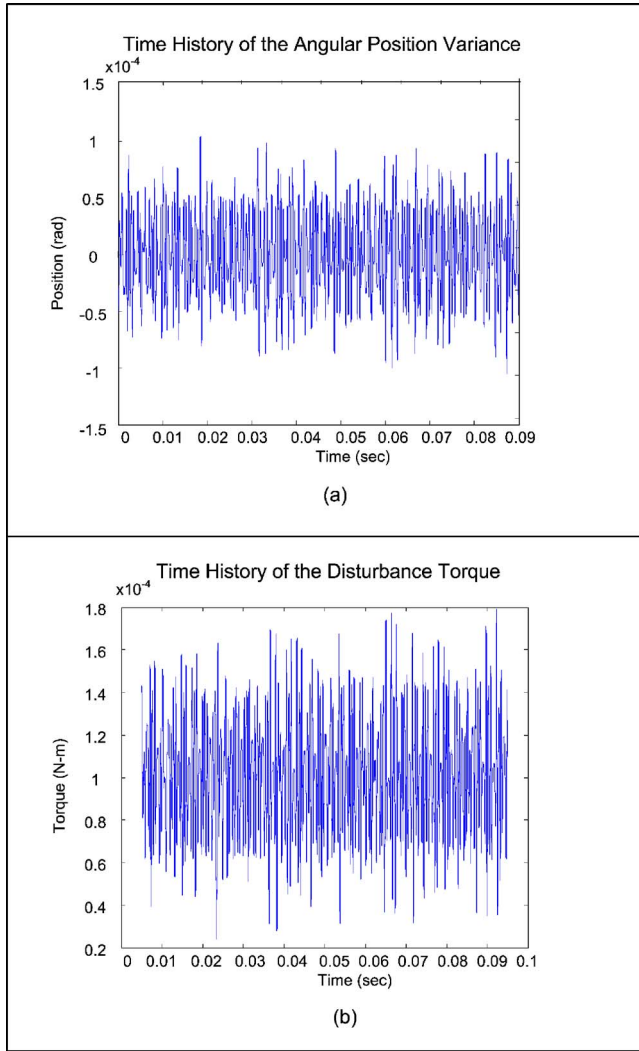


Fig. 6 Time history of the (a) angular position variance (b) disturbance torque variance

$$\mathbf{y}(t) = \mathbf{C}_{zd}\mathbf{x}(t) \quad (10)$$

can be represented. Solution of the following steady-state Lyapunov equation leads to the state covariance matrix  $\Sigma_q$ .

Table 1 Effective mass moment of inertia and effective stiffness terms for the torsional mode of the scanner

Effective moment of inertia <sup>a</sup>
$J_{\text{eff}} = J_{m,xx} + \frac{2}{3}J_{f,xx}$ $J_{f,xx} = \frac{1}{3}M_f(a^2 + b^2)$
Effective stiffness
$k_{\text{tors}} = \frac{2GK}{L_f}, \mu = \sqrt{G_{xz}/G_{xy}}$ $GK = \begin{cases} (ab^3G_{xy}) \left[ 5.33 - 3.36 \frac{b}{a\mu} \left( 1 - \frac{b^4}{12a^4\mu^4} \right) \right] & a\mu \geq b \\ (ab^3G_{xy}) \left[ 5.33 - 3.36 \frac{a\mu}{b} \left( 1 - \frac{b^4}{12a^4\mu^4} \right) \right] & a\mu < b \end{cases}$

<sup>a</sup>For mass moment of inertia terms check Table 2.

Table 2 Mass and mass moment of inertia terms for a rectangular mirror geometry

Mirror mass	Mass moment of inertia
$M_m = \rho L_m D t_m$	$J_{m,xx} = \frac{M_m}{12}(D^2 + t_m^2)$

$$\mathbf{A}_{zd}\Sigma_q + \Sigma_q\mathbf{A}_{zd}^T + \mathbf{B}_{zd}\mathbf{B}_{zd}^T = 0 \quad (11)$$

This is a matrix equation with the unknown matrix  $\Sigma_q$ , and solution techniques are available through standard commercial software packages, such as MATLAB.

The performance covariance matrix is given by

$$\Sigma_z = \mathbf{C}_{zd}\Sigma_q\mathbf{C}_{zd}^T \quad (12)$$

and the root-mean-square (rms) values of the performance metrics can be obtained from the square roots of the diagonal entries of the matrix

$$\Sigma_z = \begin{bmatrix} \sigma_{z1}^2 & \sigma_{z1z2} & \cdots & \sigma_{z1zn} \\ \sigma_{z2z1} & \sigma_{z2}^2 & \cdots & \sigma_{z2zn} \\ \vdots & \vdots & \ddots & \vdots \\ \sigma_{znz1} & \sigma_{znz2} & \cdots & \sigma_{zn}^2 \end{bmatrix} \quad (13)$$

Using the Lyapunov approach, rms estimates (in the sense of statistical steady state) can be calculated easily and directly by solving a single matrix equation. It provides the exact mean-square values of the performance variables subject to the accuracy of the disturbance and plant models. The diagonal terms of  $\Sigma_z$  represent the mean-square values  $\sigma_{zi}^2$ , and the rms values are simply  $\sigma_{zi}$  [19]. The rms value for the mirror is found to be  $1.75 \times 10^{-8}$  rad under the measured disturbance torque.

There are some shortcomings of the presented Lyapunov approach; first of all, it does not provide any direct insight into the frequency content of the outputs. Rather, it yields the overall variances of the states and the outputs. In addition to that, the solution time for the Lyapunov equation can be excessive for large-order systems. In such cases, model reduction should be performed first to bring the number of states to a reasonable level without sacrificing the predictive capability of the model.

#### 4 Sensitivity Analysis Framework

Determining sensitivity of design parameters can provide useful information when the system does not meet the specified requirements. For systems with many design parameters, sensitivity information can identify which parameters in the system are the most significant. These parameters might be the focus of redesign efforts that attempt to improve the performance.

This section describes the mathematical theory for computing sensitivities when the system is written in state-space form.

In order to compute the sensitivities, the following expression must be evaluated:

$$\frac{\partial \sigma_{zi}}{\partial p} = \text{sensitivity of a performance rms}$$

$$\text{with respect to parameter } p \quad (14)$$

The first step is to find the derivative of the variance  $\sigma_{zi}^2$  with respect to  $p$ . Taking the derivative of Eq. (12) with respect to  $p$  is

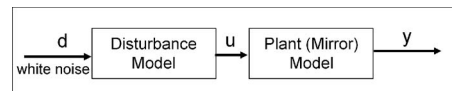


Fig. 7 Disturbance shaping filter connected in series with the mirror model

not possible because  $\Sigma_q$  is the solution to Eq. (11); therefore,  $\Sigma_q$  is implicitly dependent on  $p$ . To get around this problem, it is possible to use the Lagrange multiplier method, treat the Lyapunov equation Eq. (11) as a constraint equation, and augment it to Eq. (12) with the help of a symmetric Lagrange multiplier matrix. As suggested by Gutierrez [19], we are going to separate the problem into two sections. The first one would be to perform the modal parameter sensitivity analysis and the second would be the physical parameter sensitivity analysis.

**4.1 Modal Parameter Sensitivities Using Analytical Approach.** While the modal sensitivities do identify which modes are the most important, they do not reveal directly what physical characteristics of the design should be modified to affect the modes and improve the design. The sensitivity calculation with respect to a modal parameter is the first step to calculate the physical parameter sensitivities. In this study, the modal parameter is chosen to be the  $j$ th natural frequency  $\omega_j$ . Since the state-space system is constructed in the modal form, it is easy to calculate the system sensitivities with respect to the modal parameters.

The system matrix  $A_{zd}$  in Eq. (11) can be written as follows:

$$A_{zd} = \begin{bmatrix} \mathbf{A} & \mathbf{B}C_d \\ \mathbf{0} & A_d \end{bmatrix} \quad (15)$$

where  $\mathbf{A}$  is the plant matrix in Eq. (2).

It can be easily differentiated with respect to the modal parameter  $\omega_j$  (i.e.,  $j=1$ ).

$$\frac{\partial A_{zd}}{\partial \omega_1} = \begin{bmatrix} 0 & 0 & 0 & 0 & \dots & \dots \\ -2\omega_1 & -2\zeta_1 & 0 & 0 & \dots & \dots \\ 0 & 0 & 0 & 0 & \dots & \dots \\ 0 & 0 & 0 & 0 & \dots & \dots \\ \dots & \dots & \dots & \dots & \dots & \dots \\ \dots & \dots & \dots & \dots & \dots & \dots \end{bmatrix} \quad (16)$$

The matrix derivatives with respect to  $\omega_j$  consist entirely of zeros except at the location where those specified modal parameters appear.

The only state-space element including a modal element is the  $\mathbf{A}$  matrix: therefore, the sensitivity solution reduces to [19]

$$\frac{\partial \sigma_{zi}}{\partial p} = \frac{1}{2\sigma_{zi}} \text{trace} \left[ L_i \cdot \left( \frac{\partial A_{zd}}{\partial p} \Sigma_q + \Sigma_q \frac{\partial A_{zd}^T}{\partial p} \right) \right] \quad (17)$$

where  $\Sigma_q$  is the steady state covariance matrix, which is the solution of the Lyapunov equation (Eq. (11)) and “trace” is the summation of the diagonal terms of the matrix shown in the brackets.  $L_i$  is the Lagrange multiplier obtained by treating the Lyapunov equation as a constraint equation.

In order to compare sensitivities taken with respect to parameters of different units or magnitudes, the normalized sensitivities are computed as follows:

$$\frac{\partial \sigma_{zi} / \sigma_{zi \text{ nom}}}{\partial \omega / \omega_{\text{nom}}} = \frac{\partial \sigma_{zi}}{\partial \omega} \cdot \frac{\omega_{\text{nom}}}{\sigma_{zi \text{ nom}}} \approx \frac{\Delta \sigma_{zi}}{\Delta \omega} \cdot \frac{\omega_{\text{nom}}}{\sigma_{zi \text{ nom}}} \approx \frac{\% \text{ change in } \sigma_{zi}}{\% \text{ change in } \omega} \quad (18)$$

Results obtained for the modal sensitivity analysis of mirror are shown in Table 3. The first mode analytical sensitivity is  $-1.73$ , which means if the first natural frequency of the mirror is increased by an amount of 1%, it will result in a 1.73% decrease in the performance rms value.

If Table 3 is observed carefully, one can easily say that the first mode’s sensitivity is significantly larger than the others. Additionally, the second and third modes’ sensitivities are close to each other and they are much larger than the fourth, fifth, and sixth modes. This is an expected result if we observe the transfer function plot that relates the mirror rotation output to the given torque disturbance input in Fig. 3. The first mode of the scanner at

**Table 3 Modal parameter sensitivity analysis results of torsional scanner. Analytic solution and finite difference solution techniques are compared**

	Analytic solution (%)	Finite difference (%)
First mode sensitivity	-1.73	-1.73
Second mode sensitivity	-1.38E-5	-1.38E-5
Third mode sensitivity	-1.16E-6	-1.15E-6
Fourth mode sensitivity	3.81E-15	0
Fifth mode sensitivity	1.71E-16	0
Sixth mode sensitivity	-1.83E-16	0

5578 Hz is very dominant so performance is very sensitive to this mode. From the transfer function plot, it can be seen that the second and third torsional modes are also dominating at higher frequencies and they both have similar gains. The same trend is observed for the second and third torsional mode sensitivities in Table 1. The fourth, fifth, and sixth torsional modes are not observed in the transfer function plot and their sensitivities are close to zero.

**4.2 Modal Parameter Sensitivities Using Finite Difference Approach.** Instead of computing the sensitivity exactly, another approach is to approximate the derivative with a finite difference method. The finite difference technique is used in the modal and physical parameter sensitivity calculations as an alternative method to the exact solution. In the modal parameter sensitivity analysis, the natural frequency value is perturbed, Lyapunov equations are solved both for perturbed and unperturbed cases, and the difference of the performances is calculated. This difference of the two performance metrics is then divided by the perturbed parameter step size and the sensitivity value is approximated.

$$\frac{\sigma_{zi} - \sigma_{zi \text{ perturbed}}}{\omega - \omega_{\text{perturbed}}} = \frac{\Delta \sigma_{zi}}{\Delta \omega} \quad (19)$$

Modal parameter sensitivities calculated by finite difference method are also listed in Table 3. As it can be observed from the tabulated results, they all show good correlation between the finite difference and analytical values.

**4.3 Physical Parameter Sensitivities.** If the nominal design of a MEMS device fails to meet specified requirements, the physical parameters can be modified to improve the performance of the system. Especially for the systems with many design parameters, it is very difficult to identify the critical parameters that would affect the performance of the system. When the physical parameter sensitivity information is available, it becomes easier to identify the redesign parameters.

If sensitivity is calculated with respect to a physical parameter  $p$ , it will not appear explicitly in the state-space matrices  $A_{zd}$ ,  $B_{zd}$ , and  $C_{zd}$ .

It requires the derivative of state-space matrices with respect to modal parameters (frequencies and mode shapes), and also the frequency and mode shape derivatives with respect to physical parameter. These derivatives can be computed exactly using the methods developed by Fox and Kapoor [20] and Nelson [21].

The eigenvalue derivative can be determined by obtaining the derivatives of mass and stiffness matrices with respect to physical parameter  $p$ . One difficulty arises here since the stiffness and mass matrices are not very easy to obtain for larger-order systems. Computation of mode shape derivatives is even more complicated.

Considering the amount of computation time required to calculate the natural frequency and mode shape derivatives, analytical method is not found to be suitable for our sensitivity analysis. Instead, finite difference method is used for the calculation of the

**Table 4 Physical parameter sensitivity analysis of the torsional MEMS scanner**

	Computed normalized sensitivity
Flexure width ( $w$ )	-1.49
Flexure thickness ( $t$ )	-1.49
Flexure length ( $L$ )	0.75
Elastic modulus ( $E$ )	-0.75
Density	-0.25
Mirror thickness ( $t_m$ )	-0.25
Mirror width ( $w_m$ )	-0.25
Mirror height ( $h_m$ )	-0.74

physical parameter sensitivities of the torsional MEMS scanner.

The box shaped flexures of the scanner (see Fig. 2) are the main design variables when the stiffness of the system is considered. We performed the physical sensitivity analysis on the design variables shown in Fig. 2 using the finite difference approach. The physical parameters are perturbed one at a time in the finite element analysis, the state space model is reconstructed for the perturbed system, and the performance is calculated using the Lyapunov approach. The performance difference between the perturbed system and the original system is then divided by the perturbed parameter step size and the sensitivity value is approximated. Table 4 tabulates the physical parameter sensitivities for the torsional MEMS scanner.

Among the computed sensitivities, the greatest sensitivity belongs to the flexure beam width and thickness. An increase of 1% in the flexure width or thickness will result in 1.49% decrease in the rms performance value. Since the performance is defined as the deviation of the mirror tilt angle under random disturbances, increasing the beam thickness or width results in an increase in system stiffness and a decrease in this deviation. For the flexure beam length, it is the adverse effect. Increasing the flexure length by 1% results in a better performance by an amount of 0.75%. The flexure parameters, such as width and thickness, are suitable for redesign; however, changing the length of the flexure may not always be possible due to spacing problems. The mirror dimensions are directly related to optical resolution of the system so they are not generally included in the structural redesign efforts. However, the sensitivity results show that they are as significant as the flexure dimensions in terms of determining the performance of the torsional scanner.

## 5 Discussion and Conclusion

In this study, we developed an integrated design approach that incorporates modeling and analysis tools for analyzing system performance, sensitivity of design parameters, and critical components of MEMS devices. We demonstrated the use of the developed methodology through a case study which includes the disturbance and sensitivity analysis of a MEMS scanner mirror.

The MEMS scanner mirror is modeled using the commercial FEM software, ANSYS. Modal analysis module of ANSYS was used to obtain the mode shapes and natural frequencies of the system. The FEM results were then transferred to MATLAB in order to build the state model of the mirror to investigate the input and output relations for transfer functions. Inputs are defined as torque disturbances acting on the mirror and outputs are the amount of variance about the mirror rotation axis. This variance should be kept as small as possible in order to improve the performance of the scanner mirror.

Disturbance analysis and sensitivity analysis with Lyapunov approach take a great amount of time if large scale systems are used. Therefore, some model reduction techniques are performed to reduce the size of the FEM. The reduced model is used in the performance prediction and sensitivity analysis studies.

The performance prediction methodology uses Lyapunov equations in disturbance analysis and calculates the rms value of the angular displacement, which defines the performance of the scanning mirror. The Lyapunov approach is found to be a very efficient and accurate method. The disturbances used in the disturbance analysis framework are obtained experimentally. An experimental setup was built to measure the disturbances on the scanner mirror. An experimental procedure was developed to calculate the magnitude level of the disturbances acting on the system.

The sensitivity analysis framework is built on the disturbance analysis framework. First, the exact modal parameter sensitivities are calculated and validated with the results of the finite difference method. Modal parameter sensitivities are able to identify which modes are the most important; however, they do not provide any information regarding what physical characteristics of the design should be modified to affect the modes and improve the design. The finite difference method is used to calculate the physical parameter sensitivities and we concluded that the flexure dimensions play an important role in determining the performance of the mirror.

Sensitivity analysis tool is an extremely valuable tool especially when the MEMS system has many design parameters. One can easily identify the most significant design parameters that may affect the performance of the system. Then the designer can focus on these parameters to improve the performance.

This paper summarizes our initial attempt to create a design and analysis tool for MEMS devices. The disturbance analysis framework provides the means for predicting the performance of such systems in a very efficient and accurate way. The sensitivity analysis framework is very valuable for diagnosing the problematic components that degrade the overall system performance. All the governing equations are written in MATLAB code, which provides any easy way for further additions to the design tool. An automated routine was developed to generate the state-space model from the results of the FEM. This routine can be applied to other MEMS devices to perform disturbance and sensitivity analysis. The sensitivity analysis can be extended and then be used to perform a simultaneous optimization routine. In this study, we investigated the disturbances only for scanner mirrors. Since most of these disturbances are sensor and electronics dependent, other MEMS devices can be also studied to develop various disturbance models.

## References

- [1] Clark, J. V., Zhou, N., and Pister, K. S. J., 1998, "MEMS Simulation Using SUGAR v0.5," *Proceedings of Solid State Sensors and Actuators Workshop*, pp. 191-196.
- [2] ANSYS Release 8.1 Manual.
- [3] Li, H., and Antonsson, E. K., 1998, "Evolutionary Techniques in MEMS Synthesis," *Proceedings of ASME International Mechanical Engineering Congress and Exposition*, Anaheim, CA, Nov.
- [4] Mukherjee, T., and Fedder, G. K., 1997, "Structured Design of Microelectromechanical Systems," *Proceedings of Design Automation Conference, 34th Conference on DAC'97*.
- [5] Zhou, N., Agogino, A., and Pister, K. S. J., 2002, "Automated Design Synthesis for Micro-Electro-Mechanical Systems (MEMS)," *Proceedings of the DETC 2002: Design Automation*, Montreal, Canada.
- [6] Deshpande, M., and Saggere, L., 2005, "Modeling and Design of an Optically Powered Microactuator for a Microfluidic Dispenser," *J. Mech. Des.*, **127**(4), pp. 825-836.
- [7] Shi, F., Ramesh, P., and Mukherjee, S., 1995, "Simulation Methods for Micro-Electro-Mechanical Structures (MEMS) With Application to a Microtweezer," *Comput. Struct.*, **56**(5), pp. 769-783.
- [8] Allen, M., Raulli, M., Maute, K., and Frangopol, D. M., 2004, "Reliability-Based Analysis and Design Optimization of Electrostatically Actuated MEMS," *Comput. Struct.*, **82**, pp. 1007-1020.
- [9] Sigmund, O., 2001, "Design of Multiphysics Actuators Using Topology Optimization—Part I: One Material Structures," *Comput. Methods Appl. Mech. Eng.*, **190**(49), pp. 6577-6604.
- [10] Lusk, C. P., and Howell, L. L., 2006, "Design Space of Single-Loop Planar Folded Micro Mechanisms With Out-of-Plane Motion," *J. Mech. Des.*, **128**(5), pp. 1092-1100.
- [11] Ataman, C., 2004, "Design, Modeling and Characterization of Electrostatically Actuated Microscanners," Master thesis, Koc University.

- [12] Urey, H., and Dickensheets, D. L., 2004, *Display and Imaging Systems*, MOEMS and Applications, SPIE, Bellingham, WA, Chap. 8.
- [13] Shabana, A. A., 1991, *Theory of Vibration*, Springer-Verlag, New York, Vol. 2.
- [14] Hatch, M. R., and Raton, B., 2001, *Vibration Simulation Using MATLAB and ANSYS*, Chapman and Hall CRC, London.
- [15] Polytec Portable Digital Vibrometer, PDV 100, Manual.
- [16] Urey, H., Kan, C., and Davis, W., 2005, "Vibration Mode Frequency Formulae for Micromechanical Scanners," *J. Micromech. Microeng.*, **15**, pp. 1713–1721.
- [17] Millonas, M. M., 1994, "Transport and Current Reversal in Stochastically Driven Ratchets," *Phys. Lett. A*, **185**(1), pp. 65–69.
- [18] Gaji'c, Z., and Qureshi, M. T. J., 1995, *Lyapunov Matrix Equation in System Stability and Control*, Academic Press, San Diego.
- [19] Gutierrez, H. L., 1999, "Performance Assessment and Enhancement of Precision Controlled Structures During Conceptual Design," Ph.D thesis, Massachusetts Institute of Technology.
- [20] Fox, R. L., and Kapoor, M. P., 1968, "Rates of Change of Eigenvalues and Eigenvectors," *AIAA J.*, **6**, pp. 2426–2429.
- [21] Nelson, R. B., 1976, "Simplified Calculations of Eigenvector Derivatives," *AIAA J.*, **14**, pp. 1201–1205.